Solar cells

DOI: 10.1002/anie.201206219

Highly Efficient p-Type Dye-Sensitized Solar Cells based on Tris(1,2-diaminoethane)Cobalt(II)/(III) Electrolytes**

Satvasheel Powar, Torben Daeneke, Michelle T. Ma, Dongchuan Fu, Noel W. Duffy, Günther Götz, Martin Weidelener, Amaresh Mishra, Peter Bäuerle, Leone Spiccia, and Udo Bach**

The projected low manufacturing costs of dye-sensitized solar cells (DSCs) has made them attractive alternatives to traditional solar cells.[1] In the conventional photoanodic DSCs (n-DSCs), photocurrent generation results from dye-sensitized electron injection into n-type semiconductors, such as TiO_2. In contrast, for dye-sensitized photocathodes (p-DSC), electron transfer takes place from the valence band of the p-type semiconductor (NiO being the most commonly used to date) to the photoexcited dye.[2] The prospect of using p-DSCs as components in dye-sensitized tandem devices (pn-DSCs) has recently generated renewed interest in p-DSCs.[3] Photocathodes employing the most efficient p-DSC sensitizer (PMI-6T-TPA; see Figure 1) reported to date in conjunction with a mesoporous NiO nanoparticles film and an I^-/I_3^- based electrolyte achieved efficiencies of up to 0.41% under simulated sunlight (1000 $W m^{-2}$, AM 1.5 G). The PMI-6T-TPA-sensitized photocathode exhibits open-circuit voltages (V_{OC}) of up to 218 mV and short-circuit current densities (J_{SC}) of up to 5.35 $mA cm^{-2}$. Absorbed photon to charge carrier conversion efficiencies (APCE) up to 96% have been observed for these p-DSCs.[3] Despite this major advancement, p-DSCs are still lagging behind their n-type counterparts. Low open-circuit potentials represent a major performance limitation of these p-DSCs. Their V_{OC} is defined by the difference of the quasi-Fermi-level in the p-type semiconductor and the redox potential of the electrolyte. Strategies to increase the overall V_{OC} of p-DSCs, therefore, involve either a fine-tuning of the electronic properties of NiO, the replacement of NiO with a p-type material with a higher ionization potential or the replacement of I^-/I_3^- with a redox mediator

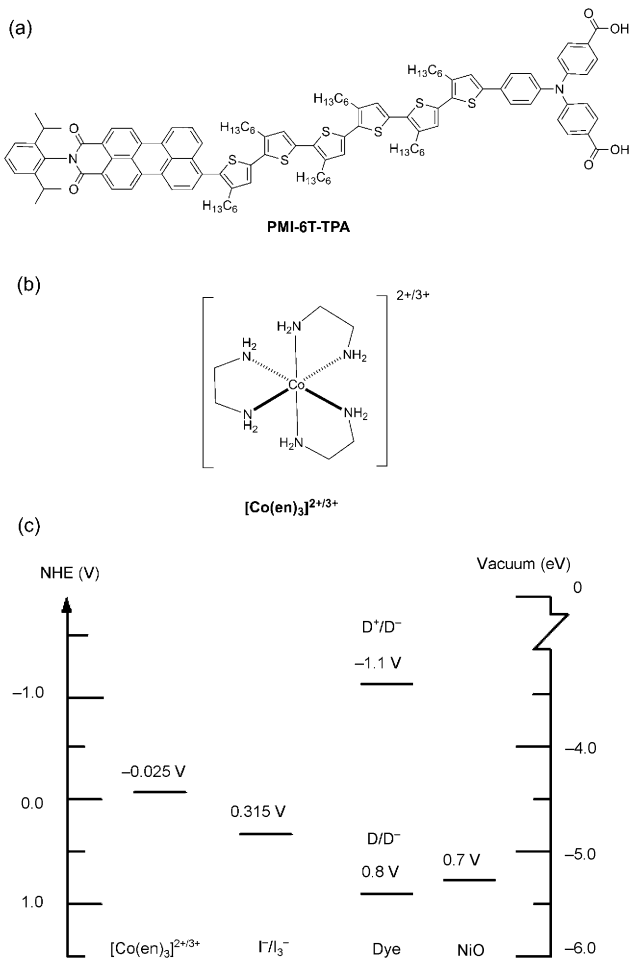

Figure 1. a) Structure of the PMI-6T-TPA sensitizer b) $[Co(en)_3]^{2+/3+}$ and c) schematic energy diagram of the p-DSC device components used in this study (D = dye; NHE = normal hydrogen electrode). Electrolyte redox potentials were measured according to reference.[7] The valence band edge of NiO was measured using photoelectron spectroscopy (PESA).

[*] S. Powar, T. Daeneke, M. T. Ma, Prof. L. Spiccia
School of Chemistry, Monash University
Clayton, Victoria 3800 (Australia)
E-mail: leone.spiccia@monash.edu
Dr. N. W. Duffy, Prof. U. Bach
Commonwealth Scientific and Industrial Research Organization, Materials Science and Engineering
Clayton South, Victoria 3169 (Australia)
Dr. G. Götz, M. Weidelener, Dr. A. Mishra, Prof. P. Bäuerle
Institute for Organic Chemistry II and Advanced Materials, University of Ulm
Albert-Einstein-Allee 11, 89081 Ulm (Germany)
D. Fu, Prof. U. Bach
Department of Materials Engineering, Monash University
Clayton, Victoria 3800 (Australia)
E-mail: udo.bach@monash.edu
Prof. U. Bach
Melbourne Centre for Nanofabrication
151 Wellington Road, Clayton, VIC 3168 (Australia)

[**] We acknowledge the Australian Research Council for providing equipment and fellowship support and the Australian Solar Institute, the Victorian State Government (DBI-VSA and DPI-ETIS) for financial support. The Commonwealth Scientific and Industrial Research Organization is acknowledged for providing support through an OCE Science Leader position (U.B.).

Supporting information for this article is available on the WWW under http://dx.doi.org/10.1002/anie.201206219.

that is more easily oxidized. Some progress in this direction was recently achieved through the use of more crystalline NiO ($V_{OC}=350$ mV), p-type semiconductors with larger ionization energy, such as $CuAlO_2$ ($V_{OC}=333$ mV), $CuGaO_2$ ($V_{OC}=357$ mV) and the use of alternative electrolytes.[4] In particular cobalt(II/III) complexes, such as $[Co(ttb\text{-}tpy)_2]^{2+/3+}$, $[Co(dMeO\text{-}bpy)_3]^{2+/3+}$, $[Co(dtb\text{-}bpy)_3]^{2+/3+}$, and $[Co(dm\text{-}bpy)_3]^{2+/3+}$ (ttb-tpy = 4,4′4″-tri-*tert*-butyl tripyridine, dMeO-bpy = 4,4′-dimethoxyl bipyridine, dtb-bpy = 4,4′-di-*tert*-butyl bipyridine, and dm-bpy = 4,4′4″-dimethyl bipyridine) have found application in p-DSCs, affording open-circuit potentials of up to 350 mV.[5] However, none of these approaches has resulted in an overall increase in energy conversion efficiency of p-DSCs beyond the 0.5% mark. Herein we report the use of tris(1,2-diaminoethane)cobalt(II/III) complexes ($[Co(en)_3]^{2+/3+}$) as redox mediators in p-DSCs. Application of this redox couple resulted in more than a twofold increase in photocathode efficiency (1.3%) and a twofold increase in V_{OC} (709 mV) compared to previously reported values.[2b,3,4,5b,6] Importantly, a J_{SC} of 4.44 mA cm^{-2} was also produced when I^-/I_3^- electrolytes were replaced by $[Co(en)_3]^{2+/3+}$ based electrolytes.

The redox potential of $[Co(en)_3]^{2+/3+}$ based electrolytes is about 340 mV more negative than that of typical I^-/I_3^- based p-DSC electrolytes, offering the scope to dramatically increase the V_{OC} of p-DSCs. At the same time, the driving force for dye-regeneration is still high (more than 1.0 eV) when $[Co(en)_3]^{2+/3+}$] electrolytes are used in conjunction with PMI-6T-TPA as sensitizer.

Three electrolytes (EL1, EL2, and EL3, see Table 1) were prepared as described in the Experimental Section. The photovoltaic performances of p-DSCs with these three different electrolytes were measured under simulated sunlight (AM 1.5 G) with different light intensities. Table 1 summarizes the photovoltaic performance at two different light intensities (100% sun and 10% sun). Photocathodes employing a classical I^-/I_3^- electrolyte (EL1) generated a V_{OC} of 284 mV with a J_{SC} of 5.35 mA cm^{-2} yielding 0.56% conversion efficiency at 100% sun condition. Replacing EL1 with the $[Co(en)_3]^{2+/3+}$ based electrolytes (EL2, EL3) resulted in a 2.3 and 2.8-fold increase in device performance at 100% and 10% sun illumination, respectively. Photocathodes using EL2 produced the highest V_{OC} of 709 mV with an efficiency of 1.3%. This corresponds to a 2.5-fold increase in V_{OC} compared to EL1 based devices. A higher concentration of LiTFSI (0.5 M) in the EL3 electrolyte lowered both the V_{OC} (660 mV) and J_{SC} (4.35 mA cm^{-2}) values but improved the fill factor (FF = 0.46) with similar power conversion efficiency (1.30%) compared to the EL2 electrolyte containing a lower LiTFSI concentration (0.1 M).

Table 1: Photovoltaic performance of p-DSCs based on mesoporous NiO electrodes.[a]

100% Sun	EL1[b]	EL2[c]	EL3[d]
V_{OC} [mV]	284 ± 15	709 ± 10	660 ± 14
J_{SC} [mA cm$^{2-2}$]	5.35 ± 0.17	4.44 ± 0.22	4.35 ± 0.40
Fill Factor	0.37 ± 0.01	0.42 ± 0.02	0.46 ± 0.05
Efficiency [%]	0.56 ± 0.04	1.30 ± 0.09	1.30 ± 0.08
10% Sun	EL1[b]	EL2[c]	EL3[d]
V_{OC} [mV]	219 ± 15	640 ± 11	587 ± 17
J_{SC} [mA cm^{2-}]	0.66 ± 0.01	0.57 ± 0.03	0.56 ± 0.04
Fill Factor	0.40 ± 0.03	0.45 ± 0.06	0.52 ± 0.02
Efficiency [%]	0.58 ± 0.06	1.61 ± 0.13	1.67 ± 0.12

[a] Film thickness = 2.5 μm and surface area = 0.16 cm^2; sensitized with PMI-6T-TPA under simulated sunlight. All p-DSCs were tested in front-illumination mode (light incident on the dye-sensitized NiO electrode) with settling time of 1 s/10 mV for EL1 and 3 s/10 mV for EL2 and EL3 measured from positive bias to negative bias. The corresponding IV curves are shown in Figure S1. [b] EL1: (0.03 M iodine, 0.6 M 1-butyl-3-methylimidazolium iodide, 0.5 M 4-*tert*-butylpyridine, and 0.1 M guanidinium thiocyanate in 85:15 acetonitrile:valeronitrile), [c] EL2: (0.07 M $[Co(en)_3](BF_4)_3$, 0.3 M $Co(BF_4)_2{\cdot}6H_2O$, 0.1 M lithium bis(trifluoromethanesulfonylimide) (LiTFSI), 1.67 M 1,2-diaminoethane in acetonitrile) and [d] EL3: (0.07 M $[Co(en)_3](BF_4)_3$, 0.3 M $Co(BF_4)_2{\cdot}6H_2O$, 0.5 M LiTFSI, 1.67 M 1,2-diaminoethane in acetonitrile).

The J_{SC} values at lower sun intensities (10% sun) were as high as 0.57 mA cm^{-2} and 0.56 mA cm^{-2} for photocathodes based on EL2 and EL3 electrolytes. Photocathodes based on EL3 electrolytes achieved the highest FF of 0.52 and overall efficiency of 1.67% at 10% sunlight intensity. The solar cell data presented was measured with settling time of 1 s for EL1 and 3 s for EL2 and EL3, where the front bias and reverse bias efficiencies co-incite with each other. For shorter settling times, hysteresis was found to affect the results (See Supporting Information, Figure S4–S9).

The stability of the electrolytes is another important aspect to explore. Aging tests were performed on p-DSC employing EL3 electrolyte at room temperature in the dark. The efficiency improved due to improvements in FF over time. Figure S2 shows the photocathodes stability data for 624 h.

To further characterize the p-DSCs, majority charge carrier lifetimes (hole lifetimes τ_p) were measured using intensity modulated photovoltage spectroscopy (IMVS). The hole lifetime describes the average time a photogenerated hole will remain in the NiO film before it crosses the NiO–electrolyte interface and recombines with the reduced redox mediator. IMVS analysis is usually combined with intensity modulated photocurrent spectroscopy (IMPS) and charge extraction measurements. IMPS measurements allow the quantification of charge transport times in the semiconductor while charge extraction analysis can be used to identify shifts in the conduction and valence bands of the semiconductor. Similar to the TiO_2 conduction band, the NiO valence band edge is known to shift with pH value.[8] Differences in the electrolyte composition, especially the addition of excess 1,2-diaminoethane, may alter the proton activity of the electrolyte. This change can lead to a shift in the NiO valence band and a change in open-circuit voltage. We found that the capacitive nature of NiO films interfered with IMPS measurements conducted at short circuit and prohibited the determination of possible valence-band shifts and changes of the charge transport times (See Figure S3 for charge extraction data).[9]

For all further analysis, p-DSCs based on EL1 electrolytes were compared with high efficiency devices based on the EL3 electrolytes. Figure 2 shows the dependence of the hole lifetime on J_{SC}. The hole lifetimes for the EL1 and EL3 based

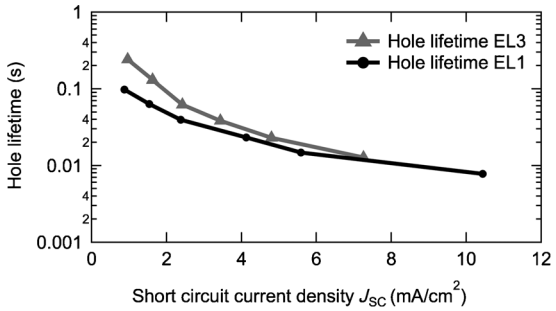

Figure 2. Hole lifetime as a function of short-circuit density (J_{SC}) for the photocathodes employing I^-/I_3^- based (black circles) and $[Co(en)_3]^{2+/3+}$ based (gray triangles) electrolytes.

devices were found to be approximately similar at a given J_{SC}, indicating similar recombination losses for I^-/I_3^- and $[Co(en)_3]^{2+/3+}$ based electrolytes. These results are encouraging since single-electron redox couples for n-DSCs usually suffer from increased recombination losses compared to two-electron redox couples.[10] Furthermore, the observed hole lifetime of 66 ms at 100 % sun is similar to electron lifetimes observed for typical high performance n-DSCs.[11]

Incident photon to electron conversion efficiency (IPCE) spectra of p-DSCs using EL3 and EL1 electrolytes are shown in Figure 3. Under front-illumination (light incident from the sensitized NiO electrode) $[Co(en)_3]^{2+/3+}$ and I^-/I_3^- based p-DSCs display almost identical IPCE spectra that feature a broad plateau between 400 and 520 nm with similar peak IPCE values of 66 % (EL1) and 57 % (EL3). To determine the redox mediator's applicability in tandem solar cells (pn-DSCs); back-illumination IPCE spectra were measured by illuminating light from the counter-electrode side. The measured IPCEs under back illumination were corrected for the transmission losses that occurred at the counter electrodes to calculate the 'corrected back-IPCEs'. The shape of the curves can easily be explained based on the absorption properties of the 22.5 μm thick electrolyte layer located between the counter electrode and the sensitized NiO film (see Figure 3 c). Above 500 nm, the corrected back-IPCEs closely follow the front IPCE for both electrolyte systems whereas below 500 nm the corrected back-IPCE of iodide based DSCs (EL1) drops down steadily to reach a value close to 0 % at about 380 nm. This drop is caused by the strong absorptivity of I^-/I_3^- based electrolytes in this wavelength range. For $[Co(en)_3]^{2+/3+}$ based DSCs (EL3), the front and corrected back IPCE follow each other closely throughout the wavelength range. At around 480 nm, the corrected back-IPCE for EL3-based DSCs shows a shallow minimum, which was not observed in front-illumination mode. This is caused by a weak absorption maximum (7.9 % absorptivity) for the $[Co(en)_3]^{2+/3+}$ electrolyte in this spectral region. Generally, the absorptivity of the $[Co(en)_3]^{2+/3+}$ based electrolyte remains well below 10 % over most of the wavelength range, making it an excellent choice for tandem solar cells where one of the two photoelectrodes inevitably needs to operate in back-illumination mode.

In conclusion, we have shown that the $[Co(en)_3]^{2+/3+}$ redox couple is an excellent mediator for p-DSCs, affording energy

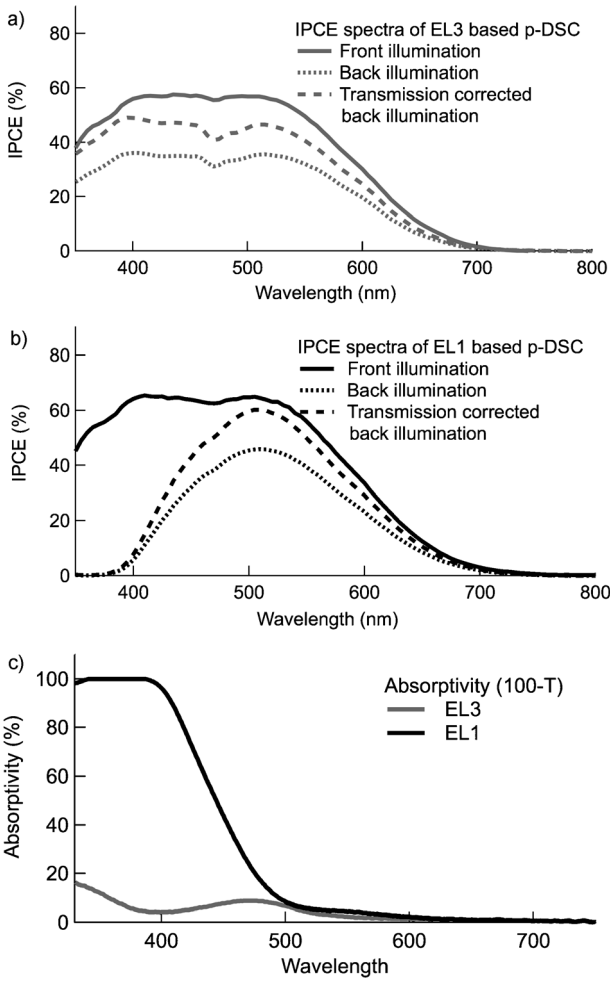

Figure 3. IPCE spectra of p-DSCs with illumination through the working electrode (front illumination), counter electrode (back illumination) and the back-illumination IPCE corrected for the transmission losses that occur at the counter electrode is also shown: a) EL3 electrolyte ($[Co(en)_3]^{2+/3+}$); and b) EL1 electrolyte (iodide/triodide) c) Absorptivity spectra of EL3 (gray line) and EL1 (black line) electrolytes in a cell with 25 μm optical pathlength. (See Experimental Section for electrolyte compositions.)

conversion efficiencies of 1.3 % at 100 % sun (1.67 % at 10 % sun) and open-circuit voltages as high as 709 mV. This corresponds to a 2.3-fold increase in η and twofold in V_{OC}, compared to the best performing p-DCSs known to date. Surprisingly, the lifetimes of photoinjected holes in the valence band of NiO were almost identical for the one-electron redox couple $[Co(en)_3]^{2+/3+}$ and the two-electron I^-/I_3^- redox system. These hole lifetimes were also comparable to the electron lifetimes in conventional TiO_2-based DSCs.

Electrolytes based on $[Co(en)_3]^{2+/3+}$ are optically transparent, making them very suitable for application in tandem solar cells, where one of the two dye-sensitized electrodes needs to operate in back-illumination mode. The use of $[Co(en)_3]^{2+/3+}$ in conjunction with dye-sensitized TiO_2 electrode, affords low built-in voltages of around 475 mV. This could provide an opportunity to develop NIR-sensitive n-DSCs, which are difficult to achieve for conventional TiO_2/dye/I^-/I_3^- DSCs owing to insufficient driving forces for either

dye regeneration or charge injection. Moreover, the use of $[Co(en)_3]^{2+/3+}$ based p-DSCs in conjunction with alternative n-type materials with higher-lying conduction band edges could provide an opportunity to realize tandem DSCs with unprecedentedly high V_{OC}.

Experimental Section

Dye-sensitized photocathodes were constructed following literature procedures.[3,12] In brief, NiO nanoparticle (Inframat) based screen-printing paste was printed on plain FTO glass (NSG—8 Ω/□, 4 mm thick) using a semi-automatic screen printer. 2.5 μm thick NiO electrodes were sensitized in a 0.2 mM PMI-6T-TPA dye solution (in DMF) for 2 h, before they were used to construct photocathodes with platinized conductive glass counter electrodes. Three electrolytes were prepared; an optimized I^-/I_3^- electrolyte (EL1); and two $[Co(en)_3]^{2+/3+}$ based electrolytes (EL2, EL3) with different LiTFSI concentrations (0.1 M and 0.5 M). The I^-/I_3^- based electrolyte (EL1) was composed of 0.03 M iodine, 0.6 M 1-butyl-3-methylimidazolium iodide, 0.5 M 4-*tert*-butylpyridine, and 0.1 M guanidinium thiocyanate in 85:15 acetonitrile:valeronitrile. The $[Co(en)_3]^{2+/3+}$ based electrolyte (EL2) contained 0.07 M $[Co(en)_3](BF_4)_3$, 0.3 M $Co(BF_4)_2{\cdot}6H_2O$, 0.1 M lithium bis(trifluoromethanesulfonylimide) (LiTFSI), 1.67 M 1,2-diaminoethane in acetonitrile. EL3 contained a higher LiTFSI concentration of 0.5 M. $[Co(en)_3]^{2+/3+}$ electrolytes were prepared in the glovebox. Exclusion of oxygen during electrolyte preparation and cell construction was important as $[Co(en)_3]^{2+}$ can oxidize to $[Co(en)_3]^{3+}$ in the presence of air.[13] Devices were characterized at slow scan rates (1 s for EL1 and 3 s for EL2 and EL3). Electrochemically deposited platinum counter electrodes were used for the front and back illumination IPCE studies.[14]

Received: August 3, 2012
Published online: November 21, 2012

Keywords: cobalt · dye-sensitized solar cells · electrolytes · photocathodes

[1] a) M. Grätzel, *Nature* **2001**, *414*, 338 – 344; b) B. O'Regan, M. Grätzel, *Nature* **1991**, *353*, 737 – 740.
[2] a) J. J. He, H. Lindstrom, A. Hagfeldt, S. E. Lindquist, *J. Phys. Chem. B* **1999**, *103*, 8940 – 8943; b) A. Morandeira, G. Boschloo, A. Hagfeldt, L. Hammarstrom, *J. Phys. Chem. B* **2005**, *109*, 19403 – 19410.
[3] A. Nattestad, A. J. Mozer, M. K. R. Fischer, Y. B. Cheng, A. Mishra, P. Bäuerle, U. Bach, *Nat. Mater.* **2010**, *9*, 31 – 35.
[4] a) X. L. Zhang, F. Z. Huang, A. Nattestad, K. Wang, D. C. Fu, A. Mishra, P. Bäuerle, U. Bach, Y. B. Cheng, *Chem. Commun.* **2011**, *47*, 4808 – 4810; b) A. Nattestad, X. Zhang, U. Bach, Y. B. Cheng, *J. Photonics Energy* **2011**, *1*, 011103; c) M. Yu, G. Natu, Z. Ji, Y. Wu, *J. Phys. Chem. Lett.* **2012**, *3*, 1074 – 1078.
[5] a) E. A. Gibson, A. L. Smeigh, L. Le Pleux, L. Hammarstrom, F. Odobel, G. Boschloo, A. Hagfeldt, *J. Phys. Chem. C* **2011**, *115*, 9772 – 9779; b) E. A. Gibson, A. L. Smeigh, L. Le Pleux, J. Fortage, G. Boschloo, E. Blart, Y. Pellegrin, F. Odobel, A. Hagfeldt, L. Hammarstrom, *Angew. Chem.* **2009**, *121*, 4466 – 4469; *Angew. Chem. Int. Ed.* **2009**, *48*, 4402 – 4405.
[6] a) A. Yella, H.-W. Lee, H. N. Tsao, C. Yi, A. K. Chandiran, M. K. Nazeeruddin, E. W.-G. Diau, C.-Y. Yeh, S. M. Zakeeruddin, M. Grätzel, *Science* **2011**, *334*, 629 – 634; b) J. F. Shi, G. Xu, L. Miao, X. Q. Xu, *Acta Phys. Chim. Sin.* **2011**, *27*, 1287 – 1299; c) P. Qin, J. Wiberg, E. A. Gibson, M. Linder, L. Li, T. Brinck, A. Hagfeldt, B. Albinsson, L. C. Sun, *J. Phys. Chem. C* **2010**, *114*, 4738 – 4748; d) P. Qin, M. Linder, T. Brinck, G. Boschloo, A. Hagfeldt, L. C. Sun, *Adv. Mater.* **2009**, *21*, 2993 – 2997; e) F. Odobel, L. Le Pleux, Y. Pellegrin, E. Blart, *Acc. Chem. Res.* **2010**, *43*, 1063 – 1071; f) A. Nakasa, H. Usami, S. Sumikura, S. Hasegawa, T. Koyama, E. Suzuki, *Chem. Lett.* **2005**, *34*, 500 – 501; g) L. Li, E. A. Gibson, P. Qin, G. Boschloo, M. Gorlov, A. Hagfeldt, L. C. Sun, *Adv. Mater.* **2010**, *22*, 1759 – 1763.
[7] G. Boschloo, L. Haggman, A. Hagfeldt, *J. Phys. Chem. B* **2006**, *110*, 13144 – 13150.
[8] a) S. Ardo, G. J. Meyer, *Chem. Soc. Rev.* **2009**, *38*, 115 – 164; b) K. Nakaoka, J. Ueyama, K. Ogura, *J. Electroanal. Chem.* **2004**, *571*, 93 – 99.
[9] a) S. K. Meher, P. Justin, G. R. Rao, *Electrochim. Acta* **2010**, *55*, 8388 – 8396; b) V. Srinivasan, J. W. Weidner, *J. Electrochem. Soc.* **2000**, *147*, 880 – 885; c) K. C. Liu, M. A. Anderson, *J. Electrochem. Soc.* **1996**, *143*, 124 – 130.
[10] a) T. Daeneke, T. H. Kwon, A. B. Holmes, N. W. Duffy, U. Bach, L. Spiccia, *Nat. Chem.* **2011**, *3*, 211 – 215; b) S. M. Feldt, E. A. Gibson, E. Gabrielsson, L. Sun, G. Boschloo, A. Hagfeldt, *J. Am. Chem. Soc.* **2010**, *132*, 16714 – 16724; c) T. Daeneke, Y. Uemura, N. W. Duffy, A. J. Mozer, N. Koumura, U. Bach, L. Spiccia, *Adv. Mater.* **2012**, *24*, 1222 – 1225.
[11] A. Zaban, M. Greenshtein, J. Bisquert, *ChemPhysChem* **2003**, *4*, 859 – 864.
[12] A. Nattestad, M. Ferguson, R. Kerr, Y. B. Cheng, U. Bach, *Nanotechnology* **2008**, *19*, 295304 – 295313.
[13] a) R. A. Krause, E. A. Megargle, *J. Chem. Educ.* **1976**, *53*, 667 – 667; b) J. A. Broomhead, F. P. Dwyer, J. W. Hogarth, *Inorg. Synth.* **1960**, *6*, 183 – 186.
[14] D. Fu, P. Huang, U. Bach, *Electrochim. Acta* **2012**, *77*, 121 – 127.

